International Journal of Nanoelectronics and Materials
Volume 12, No. 3, July 2019 [257-264]

The Effect of Sintering Temperature on Structure and Electrical Properties of $CaTiO_3$ Synthesized from Hen's Eggshell via Hydrothermal Process

Akhiruddin Maddu*[1], Nita Fitri Wahyuni[1] and Irmansyah Sofian[1]

Department of Physics, Faculty of Mathematics and Natural Sciences, Bogor Agricultural University, Dramaga, Bogor 16680, Indonesia.

Received 18 November 2018, Revised 25 January 2019, Accepted 18 February 2019

ABSTRACT

This article reports the effect of the sintering temperature on structural and electrical properties of $CaTiO_3$ synthesized via a hydrothermal route from hen's eggshell waste as a calcium source. The eggshell-derived powder was reacted with a commercial TiO_2 powder in the hydrothermal reactor then sintered in a furnace with varied temperatures. The result of X-ray diffraction analysis shows that the crystal phase of the $CaTiO_3$ samples depended on the sintering temperature. As the sintering temperature increased, the crystal phase of starting materials and secondary products decreasing, as a result, the crystal phase of $CaTiO_3$ sample to become purer. The SEM image shows that $CaTiO_3$ grains become finer and more uniform as the sintering temperature increases. The result of I-V characterization confirmed that sintering temperature greatly affected the electrical properties of $CaTiO_3$. The electrical parameter of $CaTiO_3$ samples was affected by sintering temperature, where the resistance of $CaTiO_3$ increased with the increasing sintering temperature. Whereas the resistivity of $CaTiO_3$ samples decreases with increasing sintering temperature, vice versa with the electrical conductivity.

Keywords: $CaTiO_3$, Eggshell, Electric Property, Hydrothermal, Sintering.

1. INTRODUCTION

The study of titanate-based material is currently experiencing a very rapid increase in both its properties and applications. Titanate-based materials have been well known as functional materials that were intensively studied their properties such as piezoelectric, ferroelectric, optical, and electrical properties. Titanate-based materials widely used in many application such as a gas sensor, non-volatile memories, capacitors, microwave devices, and photocatalysts [1,2]. $CaTiO_3$ is one of the titanate-based materials having a perovskite structure similar to other titanate-based compounds such as $BaTiO_3$, $PbTiO_3$, and $SrTiO_3$. $CaTiO_3$ has long been known as a material with high dielectric constants and has been applied to a variety of applications.

Because of its diverse and broad applications, several properties of $CaTiO_3$ has been studied related to its application in various fields. As the electro-ceramic materials, $CaTiO_3$ is widely studied its electrical properties to be applied in the electronic devices such as capacitors [3], non-volatile memories [4], and thermistor based temperature sensor [5]. $CaTiO_3$ is also known as microwave ceramics because it has a dielectric response in the microwave range [6]. Related to the applications for the optics and optoelectronics devices, $CaTiO_3$ has been studied extensively regarding to its optical properties [7,8]. For the development of phosphor material,

* Corresponding Author: *akhiruddin@apps.ipb.ac.id*

as for example, $CaTiO_3$ has widely been developed as a host material doped with rare-earth elements such as Eu, Pr, and Er for a luminescent generation [9-11]. Perovskite $CaTiO_3$ was also studied its capacity and capability of photocatalytic activity in degrading the organic dyes waste in the aqueous environment [12-14] and water splitting for hydrogen production in a photoelectrochemical system [15]. In addition, $CaTiO_3$ is also developed as an implant material in composite with hydroxyapatite for biomedical applications [16].

Many different methods have been developed to synthesize $CaTiO_3$ utilizing different reagents. A mechanochemical method is one of the methods used to synthesize $CaTiO_3$ from commercial powders mixture as a precursor [17, 18]. Another method to synthesize the $CaTiO_3$ powder is a microwave-assisted hydrothermal method utilizing commercial precursors such as TiO_2 and calcium salts [4, 17-21]. Other than that, $CaTiO_3$ nano-ceramics have been synthesized by high-energy ball milling method [22]. $CaTiO_3$ also has been prepared by solid-state reaction utilizing $CaCO_3$ and TiO_2 powder as starting materials [23, 24]. Each of these methods shows the uniqueness of the characteristics of $CaTiO_3$ produced including structure, morphology, and electrical and optical properties.

Most previous studies used commercial sources of calcium in the synthesizing $CaTiO_3$, such as $CaNO_3$ [12], CaO [17], $CaCl_2$ [20], and $CaCO_3$ [18, 23, 24]. In our previous study, we have synthesized $CaTiO_3$ by a hydrothermal method utilizing duck's eggshells as a source of calcium and studied the effect of sintering treatment on the structural and dielectric properties of $CaTiO_3$ produced [25]. In this study, $CaTiO_3$ was synthesized from hen's eggshells as a source of calcium by a hydrothermal method followed by a sintering process at varied temperature. The purpose of this work is to investigatethe effect of sintering treatment on the structure, morphology and electrical properties of $CaTiO_3$ synthesized by a hydrothermal method from hen's eggshell as a source of calcium instead of commercial calcium source.

2. METHODS

2.1. Synthesis of $CaTiO_3$

$CaTiO_3$ was synthesized via a hydrothermal route utilizing hen's eggshell powder obtained from the street culinary waste in Bogor City, West Java, Indonesia. While as titanium sources used commercial TiO_2 powder. Firstly, eggshell waste was cleaned from macro-contaminants by washing with deionized (DI) water then dried in the air atmosphere. Dry eggshell then was calcined at 900° C in a furnace for 5 hours with a heating rate of 5 ^oC/minute. Respectively 2 g eggshell and 2 g TiO_2 powders were mixed and ground in the mortar using pestle for 30 minutes. The mixed powder was placed into the beaker glass then 20 ml NH_4OH solution was poured into the mixture while stirred at 1000 rpm for 30 minutes. The mixture solution was transferred into the hydrothermal reactor made of Teflon, then positioned onto hotplate for the heating process. The reactor was heated at 200 ^oC for 24 hours to generate high pressure in the reactor. A white precipitate was washed several times, then dried at 100 °C for 5 hours. The dried precipitate was ground to obtain a white powder. The powder was formed into a pellet with 1.3 cm in diameter and 0.2 cm in thickness. Each pellet was sintered at a different temperature of 700 °C, 800 °C, and 900 °C for 5 hours in a furnace.

2.2. Characterization

Three samples obtained were characterized by using X-Ray Diffractometer (XRD) (SHIMADZU XRD 7000) to identify their crystal structure properties and Scanning Electron Microscope (SEM) (JEOL JSM-6360LA) to investigate their surface morphology. To explore their electrical properties, the $CaTiO_3$ pellets were characterized by using an I-V meter (Keithley 2400

Sourcemeter) to obtain current-voltage (I-V) characteristic from which the electrical parameters can be determined including resistance, resistivity, and conductivity. The $CaTiO_3$ pellet was sandwiched between two transparent conducting oxide (TCO) coated glass substrates as electrodes connected to the terminals of I-V meter.

3. RESULTS AND DISCUSSION

3.1 Crystal Structure

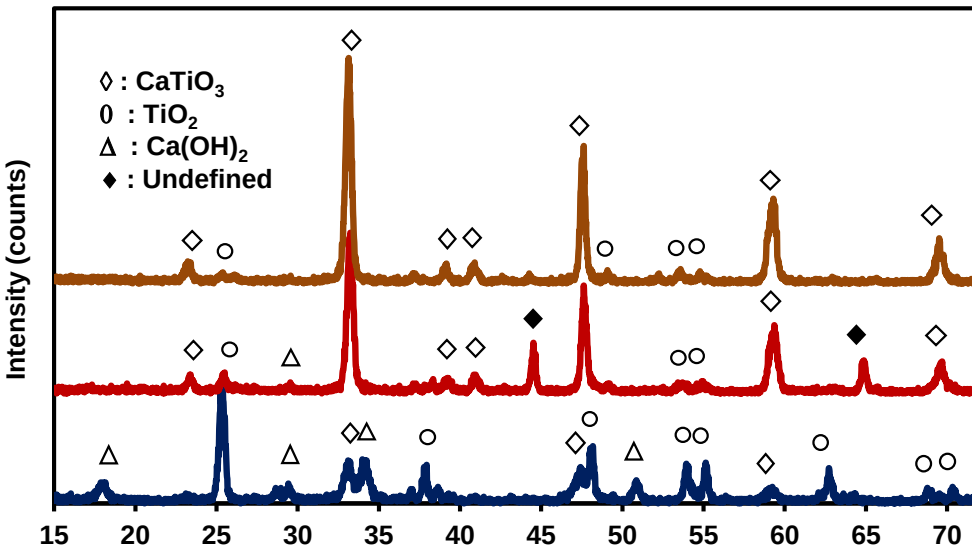

Figure 1. Diffraction spectra of $CaTiO_3$ samples with a different sintering temperature each at (A) 700 °C, (B) 800 °C and (C) 900 °C.

Investigation of crystal structure was carried out by X-ray diffraction analysis. Figure 1 shows the diffraction spectra of each sample scanned at angle 2θ from 15 to 75° for three samples of $CaTiO_3$ that were sintered at different temperatures, respectively at 700, 800 and 900 °C. There is a very significant difference between each diffraction pattern of each sample due to differences in sintering temperature, as shown in Figure 1, that indicates the sample undergo crystal phase transformation.

Based on the differences in diffraction patterns it is known that phase transformation has occurred to $CaTiO_3$ samples due to sintering treatment. Sample sintered at 700 °C shows the diffraction pattern which is still dominated by the peaks that originate from starting materials, as shown in Figure 1A. Diffraction peaks of $CaTiO_3$ were identified on the three main peaks of $CaTiO_3$ with still low intensity at 33.1 (121), 47.5 (202), and 59.3° (123), respectively. Diffraction peaks of TiO_2 anatase are still strong enough that present in the diffraction pattern, respectively at angle (2θ) 25.3° (101), 37.9° (004), 48.1° (200), 54.0° (105), 55.1° (211), 63° (204), and 69° (116), that in good agreement with the standard TiO_2 anatase (JCPDS card no. 21-1272) [26, 27]. In addition, there are also other peaks that were identified as $Ca(OH)_2$ at 18.0°, 29.4°, 34.1°, and 50.8°, respectively (JCPDS cards no. 44-1481) [28]. The presence of $Ca(OH)_2$ phase as a result of hydration of CaO. It can be concluded that sintering at 700 °C is not sufficient to cause the complete reaction between the starting materials used, that is commercial TiO_2 powder (JCPDS card no. 21-1272) and CaO from eggshells.

Sintering at 800 °C resulted in a diffraction pattern of the sample that is very different from the sample that was sintered at 700 °C, as shown in Figure 1B. The diffraction peaks of $CaTiO_3$ began to strengthen even dominate the resulting diffraction pattern, all $CaTiO_3$ peaks present in

diffraction patterns. The strongest peak of $CaTiO_3$ present at an angle (2θ) 33.1° (121), that was followed the other peaks successively at 47.5° (040), 59.3° (240), and 69.4° (242), even another weak peak also present at 23.2° (121) [28]. While the peaks of TiO_2 anatase significantly decreased even almost did not appeared, there are minor peaks of TiO_2 anatase present at 25° (101), 54.0° (105), and 55.1° (211) with very low intensity. On the other hand, a peak of $Ca(OH)_2$ also does not appear anymore. However, there are undefined peaks that appeared strong enough at the around 44° and 65° which were estimated came from intermediate products as a result of a reaction of the starting materials.

Further heating at 900 °C resulted in a diffraction pattern which has been dominated by diffraction peaks of $CaTiO_3$ phase. All the $CaTiO_3$ peaks in the diffraction pattern (Figure (1C)) was getting stronger, successively at 23.1° (101), 33.1° (121), 47.5° (040), 59.3° (042) and 69.4° (242), that in good agreement with the standard orthorhombic phase of $CaTiO_3$ (JCPDS card no. 082-0229) [24]. Even peaks that were previously not clearly seem also present at 39.1° (102) and 40.8° (220) [9, 24, 29]. The diffraction pattern obtained indicates that the $CaTiO_3$ produced more pure, similar to that produced in studies conducted by other researchers who used calcium salts as a source of calcium [9, 10, 20, 27]. Although there are still TiO_2 anatase peaks with weak intensity, these results indicate that the reaction that occurs almost perfectly to resulted in a $CaTiO_3$ compound. In this regard, it can be concluded that the optimum sintering temperature in the crystal growth of $CaTiO_3$ is at 900 °C or higher. These results can be a model in the crystal growth of $CaTiO_3$, especially those utilizing hen's eggshells as a calcium source.

3.2. Morphology

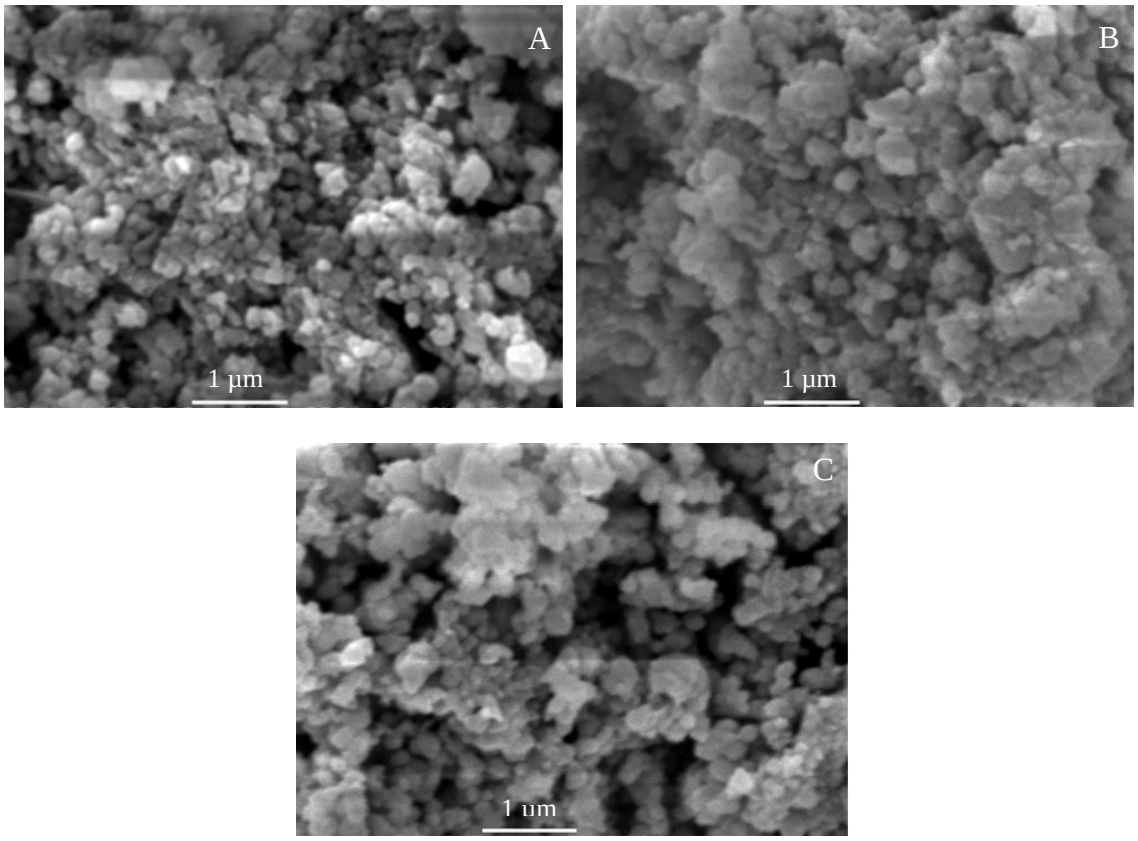

Figure 2. SEM micrograph of $CaTiO_3$ samples with different sintering temperature at (A) 700 °C, (B) 800 °C, and (C) 900 °C.

Surface morphology of $CaTiO_3$ samples was investigated by using scanning electron microscope (SEM) with a magnification of 20.000 times. Figure 2 shows SEM images of three $CaTiO_3$ samples sintered at a different temperature, that at 700 °C, 800 °C, and 900 °C, respectively. There is no significant difference in the SEM images, except that the grains of $CaTiO_3$ enlarged due to the increased in the sintering temperature. The grains look coalesce forming clots with grain boundaries are not so clear, so it is very difficult to determine the size of the grains. Sample sintered at 700 °C has a smaller grain (finer) but irregularly and size is not uniform. Sample sintered at a higher temperature of 800 °C shows the grains tend to coalesce into clumps so that looked the size becomes larger but more regularly. It is believed to be due to solid diffusion among grains in the sample sintered at higher temperatures. Sample sintered at 900 °C shows the shape of the grains more uniform that indicate the purity of $CaTiO_3$ phase in the sample. The higher the sintering temperature the stronger the diffusion of grains in the sample so as to produce granularity with higher uniformity and grains becoming clearer and finer.

3.3. Electric Property

The electrical measurement was conducted by using the I-V meter (Keithley 2400 Sourcemeter) to obtain current-voltage (I-V) characteristic of three samples sintered at a different temperature. The I-V characteristic provides information about the charge transport model in $CaTiO_3$, from which the electrical parameters of the $CaTiO_3$ sample can be determined. Measurements were made at room temperature without temperature variations, so that the effect of temperature on the electrical properties of $CaTiO_3$ was not considered. Only the effect of sintering on the electrical properties of the synthesized $CaTiO_3$ samples was considered.

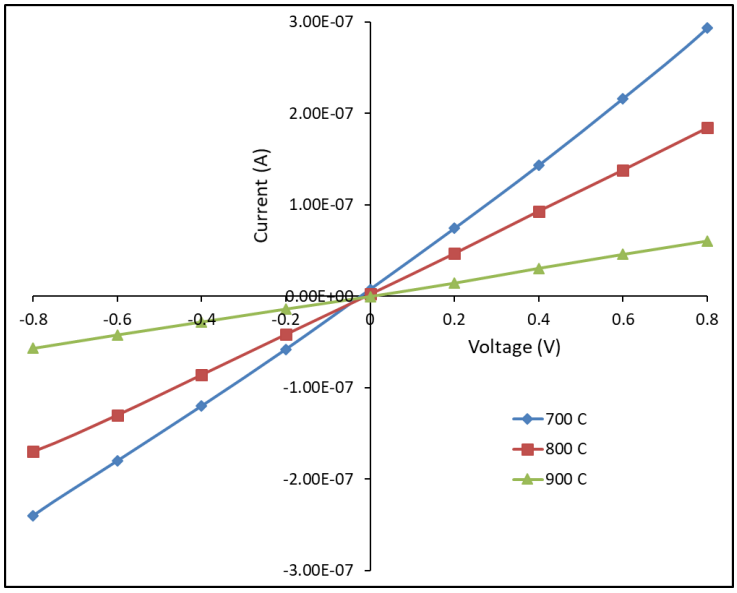

Figure 3. Current-voltage (I-V) characteristics of $CaTiO_3$ samples with different sintering temperature at 700 °C, 800 °C and 900 °C.

Figure 3 shows the current-voltage (I-V) curves of three samples of $CaTiO_3$ which were sintered at different temperature. All the I-V curves show a linear pattern in the range of -0.8 to +0.8 V which indicates the ohmic contact between the samples and the electrodes used. The three I-V characteristic curves show a different slope indicating that the samples of $CaTiO_3$ sintered at the different temperatures have different electrical characteristics. Figure 3 confirmed the resistance variation to the sintering temperature of the samples based on the different slope of I-V curves. The higher the sintering temperature the smaller the slope of the I-V curve. To determine the electrical resistance of $CaTiO_3$ samples we need to make a linear plot of I-V curves, as shown in Figure 3, in the range of -8 to +8 V. Slope ($\Delta I/\Delta V$) of the I-V curves is inverse

of the resistance (1/R), from this the resistance value can be quantitatively determined. The calculation results show that the resistance of $CaTiO_3$ increased to the increasing sintering temperature, as summarized in Table 1.

Table 1 Electrical parameters of $CaTiO_3$ sintered at different temperatures

No.	Sintering temperature (C)	Resistance (MΩ)	Resistivity (Ωcm)	Conductivity ($\Omega^{-1}cm^{-1}$)
1	700	2,778	0,184 x 10^6	5,427 x 10^{-6}
2	800	4,348	0,288 x 10^6	3,467 x 10^{-6}
3	900	13,129	0,871 x 10^6	1,148 x 10^{-6}

The resistivity value can be determined from the resistance value obtained from the I-V curve for each $CaTiO_3$ sample. With the known diameter and thickness of the samples, the resistivity of the samples can be determined based on the relation $\rho=R(A/L)$, with R is the resistance, A is the area and L is the thickness of the sample. The results of the calculation of the electrical resistivity value of each sample are summarized in Table 1, from which it is known that the resistivity of the $CaTiO_3$ sample increases with the increase in sintering temperature. The increased resistivity value of $CaTiO_3$ samples as sintering temperature increased is due to the decreased impurities in the samples. Sample sintered at 700 °C still contains significant starting materials (TiO_2 and $Ca(OH)_2$) that became impurities in the sample, as confirmed by XRD analysis. The impurities contribute to donate charges carrier in the sample so that this sample has the lowest resistivity. While, the sample sintered at 800 °C leaving only a small portion of starting material (TiO_2) that has not reacted so that relatively only a few impurities in the sample, consequently resistivity of the sample greater than the sample sintered at 700 °C. Further, in the sample sintered at 900 °C there are almost no longer impurities originating from the starting materials because it has reacted completely to be $CaTiO_3$ compound, as a result, the excess charge carrier to be greatly reduced so that the sample has a greater resistivity than the samples sintered with lower temperatures (700 °C and 800 °C).

Conversely, the electrical conductivity of $CaTiO_3$ samples decreases as the sintering temperature increases, converse with the electrical resistivity. Electrical conductivity is affected by the concentrations and mobility of the charge carrier in the sample. As perovskite crystal, $CaTiO_3$ is known as a mixed conductor which has electronic and ionic conduction [30-32]. The electronic conductivity comes from impurities that contribute to the excess negative charge (electrons) in the sample [33]. On the other hand, ionic conductivity comes from oxygen activity that contributes to electrical conductivity in the perovskite structure, including $CaTiO_3$ [31, 34]. The higher the oxygen content in the perovskite sample will potentially to increase the electrical conductivity of the sample [31]. Sample sintered at 700 °C contains more impurities cames from the starting material, that is TiO_2 and $Ca(OH)_2$ (based on XRD analysis result), that contribute enhanced oxygen content in the $CaTiO_3$ sample that plays a role in increasing oxygen activity thereby increasing ionic conductivity of $CaTiO_3$. Therefore, $CaTiO_3$ sample which was synthesized at lower temperatures has electrical conductivity higher than samples sintered at higher temperatures due to excess oxide impurities that enhanced ionic conductivity. The electrical parameter data of the $CaTiO_3$ sample were summarized in Table 1. Based on the data it can be concluded that the charge carrier which is dominant in the sample $CaTiO_3$ is an ion carrier that comes from oxygen activity due to oxygen excess in the sample.

4. CONCLUSION

$CaTiO_3$ have been successfully synthesized utilizing eggshell waste as a source of calcium via the hydrothermal process followed by sintering treatment. The crystal phase of growth $CaTiO_3$ were

greatly dependent on the sintering temperature. The crystal phase of $CaTiO_3$ increasingly dominated with increasing sintering temperature, the sample sintered at 900 ^oC is purer than the sample sintered at lower temperatures. Morphology of the $CaTiO_3$ samples also was influenced by sintering temperature, due to increasing of the sintering temperature the grains more uniform and finer. Likewise, the electrical properties of the samples are also highly dependent on the sintering temperature. The electrical resistance of $CaTiO_3$ samples increased as increasing the sintering temperature, due to decreasing the charge carriers originating from impurities in the sample. Resistivity of $CaTiO_3$ samples increases significantly to the increase in sintering temperature, whereas the electrical conductivity of the $CaTiO_3$ decreases with the increase of sintering temperature due to the decrease in impurity in the sample. Indeed, the sample with higher sintering temperatures (900 ^oC) showed the crystal phase of $CaTiO_3$ was purer, but had lower electrical conductivity, so that applications as dielectric materials were more suitable for samples sintered at lower temperatures because of their higher electrical conductivity.

REFERENCES

[1] Kimijima, T., Kanie, K., Nakaya, M. & Muramatsu, A., Mater. Trans. **55**, 1 (2014) 147-153.
[2] Sakhya, A.P., Maibam, J., Saha, S., Chanda, S., Dutta, A., Sharma, B.I., Thapa, R.K. & Sinha, T.P., Indian J. Pure and Appl. Phys. **53** (2015) 102-109.
[3] Krause, A., Weber, W. M., Phol, D., Rellinghaus, B., Verheijen, M., Mikolajick. T., ACS Appl. Mater. Interfaces **6**, 22 (2014) 19737-19743.
[4] Pashkin, A., Kamba, S., Berta, M., Petzelt, J., Csete de Dy"orgyfalva, G.D.C., Zheng, H., Bagshaw, H., Reaney, I. M., J. Phys. D: Appl. Phys. **38**, 5 (2005) 741-748.
[5] Lv, F., Gao, C., Zhang, P., Dong, C., Zhang, C., Xue, D., RSC Adv. 5, **51** (2015) 40714.
[6] Sahoo, S., Parashar, S. K. S., Ali, S. M., Eaten, D. L, J. Adv. Ceram. **3**, 2 (2014) 117-124.
[7] Moreira, M. L., Paris, E. C., Do Nascimento, G. S., Longo, V. M., Sambrano, J. R., Mastelaro, V. R., Bernardi, M. I. B., Andrés, J., Verala, J. A., Longo, E., Acta Mater. **57**, 17 (2009) 5174-5185.
[8] Cavalcante, L. S., Marques, V. S., Sczancoski, J. C., Escote, M. T., Joya, M. R., Verala, J. A., Santos, M. R. M. C., Pizani, P. S., Longo, E., Chem. Eng. J. **143**, 1-3 (2008) 299-307.
[9] Mazzo, T. M., Moreira, M. L., Pinatti, I. M., Picon, F. C., Leite, E. R., Rosa, I. L. V., Varela, J. A., Perazzoli, L. A., Longo, E., Optical Mater. **32**, 9 (2010) 990-997.
[10] Yoon, S., Otal, E. H., Maegli, A. E., Karvonen, L., Matam, S. K., Riegg, S., Ebbinghaus, S. G., Fallas, J. C., Hagemann, H., Walfort, B., Pkrant, S., Weidenkaff, A., Optical Mater. Express. **3**, 2 (2013) 248-258.
[11] Dereń, P. J., Mahiou, R., Pązik, R., Lemanski, K., Stręk, W., Boutinaud, Ph., J. Lumin. **128**, 5-6 (2008) 797-799.
[12] Huo, Y. S., Yang, H., Xian, T., Jiang, J. L., Wei, Z. Q., Li, R. S., Feng, W. J., J. Sol-Gel. Sci. Technol. **71**, 2 (2014) 254-259.
[13] Yan, Y., Yang, H., Zhao, X., Li, R., Wang, X., Mater. Res. Bull. **105** (2018) 286-290.
[14] Dong, W., Bao, Q., Gu, X., Zhao, G., J. Ceram. Soc. Jpn. **123**, 8 (2018) 643-648.
[15] Jang, J. S., Borse, P. H., Lee, J. S., Lim, K. T., Jung, O. S., Jeong, E. D., Bae, J. S., Kim, H. G., Bull. Korean Chem. Soc. **32**, 1 (2011) 95-99.
[16] Dubey, A. K., Basu, B., Balani, K., Guo, R. & Bhalla, A. S., Integrated Ferroelectrics **131**, 1 (2011) 119-126.
[17] Park, K. H., Kim, H. G., J. Korean Phys. Soc. **56**, 2 (2010) 648-652.
[18] Palaniandy, S., Jamil, N. H., J. Alloys Comp. **476** (2009) 894–902.
[19] Yan, Y., Yang, H., Zhao, X., Zhang, H., and Jiang, J., J. Electron. Mater. **47**, 5 (2018) 3045-3050.
[20] Lozano-Sańchez, L. M., Lee, S. W., Sekino, T., Rodríguez-González, V., Cryst. Eng. Comm. **15**, 13 (2013) 2359-2362.

[21] Pereira, S. C., de Figueiredo, A. T., Barrado, C. M., Stoppa, M. H., dos Santos, T. O., Pontes, F. M., Longo, E., Mater. Res. Express **4** (2017) 065014.
[22] Sahoo, S., Dash, U., Parashar, S. K. S., Ali, S. M., J. Adv. Ceram. **2**, 3 (2013) 291-300.
[23] Wu, Y., Sun, Z., Ruan, K., Xu, Y., Zhang, H., J. Lumin. **155** (2014) 269-274.
[24] Li, J., Zhang, Y. C., Wang, T. X., Zhang, M., Mater. Lett. **65** (2011) 1556-1558.
[25] Maddu, A., Permatasari, L., Arif, A., J. Ceram. Process. Res. **18**, 2 (2017) 146-150.
[26] Meng, X., Shin, D. W., Yu, S. M., Jung, J. H., Kim, H. I., Lee, H. M., Han, Y. H., Bhoraskar, V., Yoo, J. B., Cryst. Eng. Comm. **13** (2011) 3021-3029.
[27] Yang, J. W., Hu, J., J. Lumin. **145** (2014) 144-147.
[28] Alavi, M. A., Morsali, A., J. Exper. Nanosci. **5**, 2 (2010) 93–105.
[29] Shivram, M., Prashantha, S. C., Nagabhushana, H., Sharma, S. C., Thyagarajan, K., Harikrishna, R., Nagabhushana, B. M., Spectrochim. Acta Part A: Molecular and Biomol. Spectrosc. **120** (2014) 395-400.
[30] Bak, T., Nowotny, J., Sorreil, C. C., Zhou, M. F., Ionics **10** (2004) 334-342.
[31] Bak, T., Nowotny, J., Sorrel, C. C., Zhou, M. F., J. Mater. Sci.: Mater. Electron. **15**, 24 (2004) 635-644.
[32] Mather, G. C., Islam, M. S., Figueiredo, F. M., Adv. Funct. Mater. **17** (2007) 905–912.
[33] Bak, T., Burg, T., Nowotny, J., Blennerhassett, P.J., Chem. Mater. **23** (2003) 1607–1617.
[34] Hayashia, H., Inaba, H., Matsuyama, M., Lan, N. G., Dokiya, M., Tagawa, H., Solid State Ionics **122** (1999) 1–15.